



Düzce University Journal of Science & Technology

Research Article

Optimization of Hybrid Sonophotocatalytic Decolorization of Rhodamine B (RhB) Dye Using TiO₂ Nanocatalyst

 Gamze DOĞDU^{a,*}

^a*Çevre Mühendisliği Bölümü, Mühendislik Fakültesi, Bolu Abant İzzet Baysal Üniversitesi, Bolu, TÜRKİYE*

* Sorumlu yazarın e-posta adresi: gamedogdu@ibu.edu.tr

DOI: 10.29130/dubited.1022337

ABSTRACT

Rhodamine B (RhB) dye is studied as target pollutant in this work due to its various adverse effects on skin, gastrointestinal and respiration systems. In the present study, decolorization of RhB dye by sonophotocatalysis (SPC) method in a synthetic aqueous solution was investigated using a hybrid laboratory-scale, batch-mode reactor system with a pure, nano-sized catalyst under ultraviolet A (UVA) light (~365 nm) irradiation for 90 minutes. To achieve maximum RhB decolorization, independent parameters which were TiO₂ concentration (0.5 to 2.5 g/L), initial pH (2 to 10) and concentration of RhB (10 to 50 mg/L), were chosen in this method. The three-level Box-Behnken factorial design (BBD) was selected to carry out the optimization method. The finding results presented that TiO₂ concentration of 0.5 g/L, pH 2, and an initial RhB concentration of 15.25 mg/L were optimum parameters to achieve maximum RhB decolorization. Further, lamp type, lamp electrical power, and adding H₂O₂ that could affect the removal efficiency were investigated as a first time. Based on ANOVA analysis, concentration of RhB stated the most significant effects followed by pH and TiO₂ concentration on the model. A good compliance between experimental results and predictive values were obtained by the regression analysis for the model with R² value of 0.9902. The results showed that the Langmuir–Hinshelwood (L-H) model could clarify the SPC process well, where k_c and K_{LH} were 0.941 mg/Lmin and 0.129 L/mg, respectively.

Keywords: Rhodamine B (RhB), Sonophotocatalysis (SPC), Box Behnken design (BBD), Hybrid system, Decolorization

TiO₂ Nanokatalizörü Kullanarak Rodamin B (RhB) Boyasının Hibrit Sonofotokatalitik Renk Giderimi Optimizasyonu

Öz

Rhodamine B (RhB) boyası, cilt, gastrointestinal ve solunum sistemleri üzerindeki çeşitli olumsuz etkileri nedeniyle bu çalışmada hedef kirletici olarak incelenmiştir. Bu çalışmada, sentetik sulu bir solüsyonda RhB boyasının sonofotokataliz (SFK) metoduyla renk giderimi, ultraviyole A (UVA) ışığı (~365 nm) altında 90 dakikada, saf, nano boyutlu bir katalizörle hibrit laboratuvar ölçekli, kesikli mod reaktör sistemi kullanılarak araştırılmıştır. Maksimum RhB renk giderimi elde etmek için, bu yöntemde TiO₂ konsantrasyonu (0.5 ila 2.5 g/L), başlangıç pH'ı (2 ila 10) ve RhB konsantrasyonu (10 ila 50 mg/L) olan bağımsız parametreler seçilmiştir. Optimizasyon sürecini gerçekleştirmek için üç seviyeli Box-Behnken faktöriyel tasarımı (BBD) seçilmiştir. Bulunan sonuçlar, 0.5 g/L TiO₂ konsantrasyonu, pH 2 ve 15.25 mg/L başlangıç RhB konsantrasyonunun maksimum RhB renk giderimi elde etmek için optimum parametreler olduğunu göstermiştir. Ayrıca ilk defa lamba tipi, lamba elektrik gücü ve giderim verimini etkileyebilecek H₂O₂ ilavesi incelenmiştir. ANOVA analizine göre, model üzerinde RhB konsantrasyonu en önemli etkiye sahipken, bunu pH ve TiO₂ konsantrasyonu takip etmiştir. R² değeri 0.9902 olan model için regresyon analizi tarafından deneysel sonuçlar ile tahmin değerleri arasında iyi bir

uyum elde edilmiştir. Sonuçlar, Langmuir-Hinshelwood (L-H) modelinin, k_c ve K_{LH} 'ın sırasıyla 0.941 mg/Lmin ve 0.129 L/mg olduğu SFK prosesini iyi açıklayabildiğini göstermiştir.

Anahtar Kelimeler: Rodamin B (RhB), Sonofotokataliz (SFK), Box Behnken Dizaynı (BBD), Hibrit sistem, Renk Giderimi

I. INTRODUCTION

Synthetic organic dyes have colorful, complex and molecular structure that are extensively used in industries, i.e., textile, pharmaceutical, printing, cosmetics, etc. [1]. Turkey's textiles sector is on the first rank within the country, being the third in the European Union, and also it is among the seven leading textile exporters in the world, at the end of 2017 [2]. In textile processing industry, 20% of industrial wastewater is generated due to dyeing and finishing processes [3]. The synthetic and industrial dye effluents are classified as one of the most serious environmental pollutants especially in water systems due to their high oxygen demands, strong color, toxic, non-biodegradable, carcinogenic and teratogenic structure [3,4]. Water pollution caused by dyes dramatically endanger to human health and entire ecosystem and that are responsible for the perturbations for the aquatic life, esthetic pollutions [5].

Rhodamine B (RhB) is a toxic and carcinogenic xanthene dye that is extensively used in textile industries and it is dangerous due to its adverse effects such as skin and eyes irritations, carcinogenicity, reproductive disorders, respiratory and gastrointestinal diseases [6,7]. Thus, treatment of wastewater effluents containing such dye pollutants is considerably significant to prevent any detrimental effects towards whole ecosystem. Many conventional physico-chemical and biological treatment methods are used for decolorization of dyeing wastewater have various limitations [7-9]. Such limitations are high cost, slow kinetics, long treatment times, low performance, difficulty in reactor design, higher waste production and energy consumption and ineffectiveness on their degradation [4, 10]. The breakage of chromophores resulted with decolorization is the first step for the dye degradation that is monitored by a spectrophotometer (a decrease in absorbance) and expressed as the percentage of removed dye indicating only the breakage of the chromophores rather than complete mineralization [11-13]. Nevertheless, the advanced oxidation processes (AOPs) and their hybrid combinations are feasible and renewable techniques to completely degrade wastewater especially containing hardly degradable organic dye pollutants and dye's cleavage products (i.e. aromatic amines) that are more detrimental than parent compound until CO_2 and H_2O by reacting with hydroxyl radicals ($\bullet OH$) [14-16]. Recently, the coupling of photocatalysis (UV/ TiO_2) and ultrasound (US) waves called 'sonophotocatalysis' (SPC), have gained attention as a way to combine the advantages of the two processes to degrade all kinds of compounds from water owing to easy operational, cheapness, and environmental friendly [17-20]. The individual advanced oxidation methods have many drawbacks including, insufficient transmission of light in water and limited reactive oxygen species (ROS) generation that prevents several applications [21, 22]. However, several phenomena such as cavitation, nucleation and sonoluminescence due to the interaction of ultrasound with the dye solution and also the surface of solid catalyst particles are vital superiorities on the hybrid SPC process than other individual AOPs in the literature [23]. Consequently, the hybrid SPC process poses various advantages: (1) generation of additional free $\bullet OH$ radicals is increased in the reaction mixture, in the presence of catalyst (2) the ultrasonic liquid turbulence between catalyst interface and solution phase enables mass transfer between oxygen, pollutants and by-products close to the surface of catalyst, (3) catalytic activity is improved owing the ultrasound waves irradiation, (4) the required treatment time and cost can be reduced associated with an increase in energy consumption that clearly explains the reason why SPC process is preferred [7, 24-27].

To the best our knowledge, there are limited studies on the decolorization of RhB dye by combination of ultraviolet with ultrasound and TiO_2 catalyst, as compared with literature [14, 17-20]. [18] stated in their study that optimum RhB degradation was succeeded by ultrasound-assisted TiO_2 photocatalysis with 500 mg/L of TiO_2 dosage, 20 mg/L of RhB concentration, at pH 7 under 40 kHz frequency and 300 W ultrasonic power. Also, [10] explained that the maximum degradation as 91% for Rh-B was obtained

using sonophotocatalytic (US/UV/TiO₂) treatment in 180 min operation period with 10 mg/L of RhB and 0.2 g/L H₂O₂ concentration at pH 2.5. Furthermore, [19] declared that RhB was decolorized completely within a few minutes in the US/UV/TiO₂ system with 0.5 g/L TiO₂, 10 mg/L of RhB and 1 mmol/L H₂O₂ concentrations. However, conventional methods to optimize decolorization of RhB that are mentioned above could determine one variable independently at a specific time while keeping other factors constant, so they are time-consuming [28]. Response surface methodology (RSM) is a popular analytical and statistical tool by researchers to obtain optimal operating conditions especially for AOPs by creating experimental design [28, 29]. RSM also is used to evaluate the method's ability in quantifying the relation between responses and several variables [30] that also have not been discussed before for the evaluation of RhB dye decolorization by SPC method. Box-Behnken design (BBD) is a promising RSM method that is mostly used for its fast and economic specialties than traditional approaches [31]. Furthermore, there is still a big gap for application of RSM in effectively optimizing the hybrid SPC process (US-UV/TiO₂). Therefore, in this study, the performance of hybrid SPC method was successfully evaluated to treat common used dye pollutant RhB in aqueous solution. In addition, as a first time, the effect of UV lamp type and lamp's electrical power were discussed on the dye decolorization by SPC method in this study. Further, the effects of solution pH, TiO₂ catalyst and RhB concentrations, on the SPC process were examined by BBD in combination with RSM. Optimum operating conditions depends on parameter interactions were also carried out. The recommended hybrid method achieved the highest (99%) RhB dye decolorization efficiency in a short time with less number of examinations.

II. MATERIAL AND METHODS

A. CHEMICALS AND REAGENTS

The nanopowder TiO₂ (AEROXIDE[®] P25≥99.5%, anatase form, 21 nm, 35–65 m²/g BET surface area) was supplied by Sigma-Aldrich (Germany). Rhodamine B as model pollutant (C.I. Basic Violet 10, Molecular formula: C₂₈H₃₁ClN₂O₃, Color: pink, CI number: 45170, Molecular weight: 479.02 g/mol, λ_{max}: 544 nm) was supplied from Sigma-Aldrich (Germany). The molecular structure of RhB is shown in Table 1. Sodium hydroxide (NaOH, 99%), and Sulfuric acid (H₂SO₄, 97%) were procured from Merck (Germany). Hydrogen Peroxide (30%, H₂O₂) was used as an oxidant that provided by Sigma-Aldrich (Germany). During the experiments, deionized water was used to prepare necessary solutions (Merck Milli-Q (Germany), spec. resistivity: 18.2 MΩ).

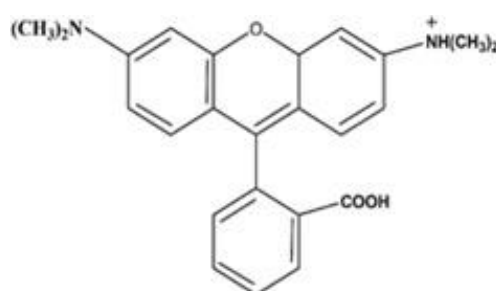


Figure 1. Characteristics of Rhodamine B (RhB) dye

B. REACTOR DESIGN AND ANALYSIS

All ultrasound, photocatalytic, and sonophotocatalytic experiments were performed using the same cylindrical Pyrex glass immersion well reactor filled with 200 mL RhB solution with certain amount of TiO₂. The batch-mode reactor equipped with a water jacket and a PL-L UVA lamps (Philips, Dutch) (9-69W; 315 to 380 nm; 110 μW/cm²) and UVC lamp (Philips, Dutch) (9 W; 254 nm) were fitted was used to study the SPC method (Figure 2). 3.5 L/min of air was supplied to the reactor system using a diffuser. The whole photoreactor system was immersed into an ultrasonic bath for the US experiments (Bandelin

DT 106, Germany) with a capacity 5.6 L (operating volume, 200 mL), a tank size of $D = 240$ mm and $L = 125$ mm, and an operating frequency of 35 ± 3 kHz (120 W, 220 V). During the experiment, the reactor temperature was kept constant at 25 ± 2 °C with a continuous water bath and a cold water pump. Optical densities of samples were measured after filtration of TiO_2 catalyst from solution.

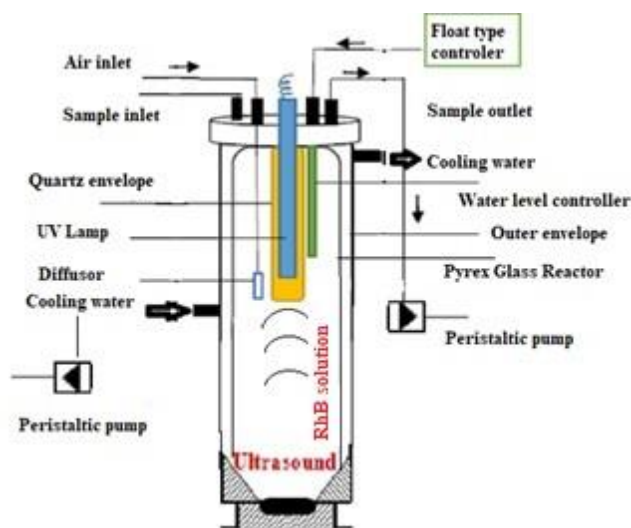


Figure 2. Experimental set up for hybrid SPC system

Optimization of SPC conditions was initially done using a spectrophotometer (Merck Pharo 100, Germany). Maximum wavelength (λ_{max}) of RhB dye was read at 544 nm and all absorbance values of samples was measured at the same wavelength. Each experiment was carried out in duplicate and their average values are presented in this work. Removal efficiency was calculated using Equation 1 [28]:

$$\text{Removal efficiency (Y)} = \left(\frac{C_0 - C}{C_0} \right) * 100 \quad (1)$$

where C_0 and C are initial RhB concentration and final concentration after distinct reaction time, respectively.

C. EXPERIMENTAL DESIGN

In the current investigation, TiO_2 concentration (X_1), pH (X_2) and initial RhB dosage (X_3) were independent variables, while decolorization efficiency of RhB dye was the dependent response variable in the SPC system. The levels and ranges of the independent variables were shown in Table 1. Previous experiments provided insights us to determine the ranges of independent variables. All analytical experiments were carried out in duplicate. Experimental data was represented by using second-order polynomials to provide the best-fit regression equations to obtain well predictions [21].

Table 1. Experimental design levels

Model	Ranges and levels		
	Low(-1)	Medium (0)	High (+1)
TiO ₂ concentration (x_1 , g/L)	0.5	1.5	2.5
pH (x_2)	2	6	10
RhB dosage (x_3 , mg/L)	10	30	50

The integrated effect of the three independent variables with 15 sets of experiments of which 3 are repetitions was evaluated using of BBD. To define model terms and to fit experimental data, a second-order polynomial equation (Equation 2) was used. Table 2 presents the experiment sets, the predicted and observed RhB decolorization. The quadratic response model could be defined as [28]:

$$Y = \beta_0 + \sum_{i=1}^k \beta_i x_i + \sum_{j=2}^k \sum_{i=1}^{j-1} \beta_{ij} x_i x_j + \sum_{i=1}^k \beta_{ii} x_i^2 \quad (2)$$

Y (%) represented the decolorization efficiency of RhB, β_0 , β_i were the interception coefficient, β_{ii} was quadratic term, β_{ij} was interception coefficient [22].

Minitab Software (v17) was used to perform regression and optimization applications. “Goodness of fit” and analysis of variance (ANOVA) techniques were performed to assess the capacity of designed models. The p value of <0.05 means a significant effect for pH, TiO₂ and initial RhB concentrations on RhB decolorization efficiencies. After all the statistical analysis, three-dimensional (3D) surface plots and two-dimensional (2D) contour plots from validated models were generated using RSM while fixing a variable constant [31]. Consequently, to achieve maximum RhB decolorization, optimum conditions of the process parameters were evaluated.

Table 2. Experimental and predicted responses for decolorization percentage of RhB

Run	Coded Levels			RhB decolorization (%)	
	X ₁	X ₂	X ₃	Experimental	Predicted
1	-1	-1	0	95.5	96.2
2	1	-1	0	87.8	86.6
3	-1	1	0	99.9	101.1
4	1	1	0	98.5	97.8
5	-1	0	0	96.3	95.6
6	1	0	0	92.9	94.1
7	-1	0	1	89.6	88.5
8	1	0	1	76.4	77.1
9	0	-1	-1	98.4	98.4
10	0	1	-1	95.4	95.0
11	0	-1	1	74.4	74.9
12	0	1	1	94.3	94.3
13	0	0	0	94.8	95.2
14	0	0	0	95.1	95.2
15	0	0	0	95.5	95.2

III. RESULTS AND DISCUSSION

A. DECOLORIZATION OF RHODAMINE B UNDER VARIOUS CONDITIONS

The system was stirred for at least 30 minutes in the dark following the addition of TiO₂ photocatalyst to produce a homogeneous suspension and to allow the system to reach equilibrium in case of adsorption-desorption. As illustrated in Figure 3, the maximum decolorization efficiency of RhB was 8.56% by catalysis at dark conditions that gives an opinion for the adsorbed RhB dye amount in the equilibrium conditions. For comparison, irradiation experiments without adding photocatalyst were also performed and 11.1% of RhB decolorization efficiency was obtained in the presence of ultraviolet irradiation UVA₃₆₅ that is called “photolysis”. Besides, individual ultrasound performance on the

decolorization of RhB dye was attained as 15.4%, suggesting the unsatisfactory treatment capabilities of individual processes. Similar to our findings, [32] stated that 8.2% of RhB was degraded under 40 kHz ultrasonic vibration in the absence of any catalyst. Our results are also in agreement with [33] who stated that RhB solution was decolorized within 2 h of ultrasonic irradiation between 200-500 kHz ultrasonic frequencies that could be explained by the fact that the lifetime of the bubbles produced at low frequencies was longer and the production of radicals was slow, compared to systems using higher frequencies. In addition, especially at low frequencies, the formation of highly hydrophilic intermediates via $\bullet\text{OH}$ attack lead to long sonochemical degradation time in order to achieve complete mineralization [19]. US-TiO₂ showed only 20.5% removal of RhB whereas coupling of US-UV could enhance the decolorization efficiency as 40.3%. The decolorization of RhB in the UV-TiO₂ system showed high removal rates of 86.9% due to the excellent activation capability of TiO₂ under UV irradiation as an efficient photocatalyst [25, 26]. Combination of US with UV and catalyst substantially promoted the decolorization efficiency of RhB (98.51%) basically. Because US conditions help to improve the dispersal of TiO₂ nanoparticles by preventing agglomeration, thus generation of radicals could be increased with higher catalyst active sections exposed [27]. Further, size reduction of photocatalyst particles consequent to particle deaggregation cause to an increase in the surface area and catalytic performance. So, US can enable to increase the photocatalytic reaction rate by the catalytic activity of the catalyst. Also, acoustic cavitation cleans the catalyst surface and mass transfer induced by US is accelerated between the solution and catalyst, which might lead to increase the photocatalytic degradation rate [20].

Besides, the decolorization of RhB was promoted in the US-UV/TiO₂/H₂O₂ depended on the improvement on H₂O₂ activation in hybrid process. The limitations of SPC process was overcome by supporting the process with H₂O₂ due to producing extra $\bullet\text{OH}$ in the presence of US and UV processes [34]. Fundamentally, adding of H₂O₂ regardless of its concentration into the SPC system couldn't improve the decolorization efficiency of RhB substantially, but it maximized the removal efficiency in a short time compared with US/UV-TiO₂ system as shown in Figure 4. Likewise, higher lamp electrical power enhanced the degradation of RhB in a short working period regardless of lamp type.

The synergistic relationship between sonocatalytic and photocatalytic processes is confirmed by various studies [26, 35]. The synergy index that is the ratio of the hybrid SPC rate constant to the sum of the individual processes' rate constants was calculated to present the contributions from UV and UV-TiO₂ processes. The synergy index was calculated as shown in Equation 3 [36]:

$$\text{Synergy (\%)} = \frac{K_{(\text{US-UV/TiO}_2)}}{K_{(\text{US})} + K_{(\text{UV/TiO}_2)}} = 2.42 \quad (3)$$

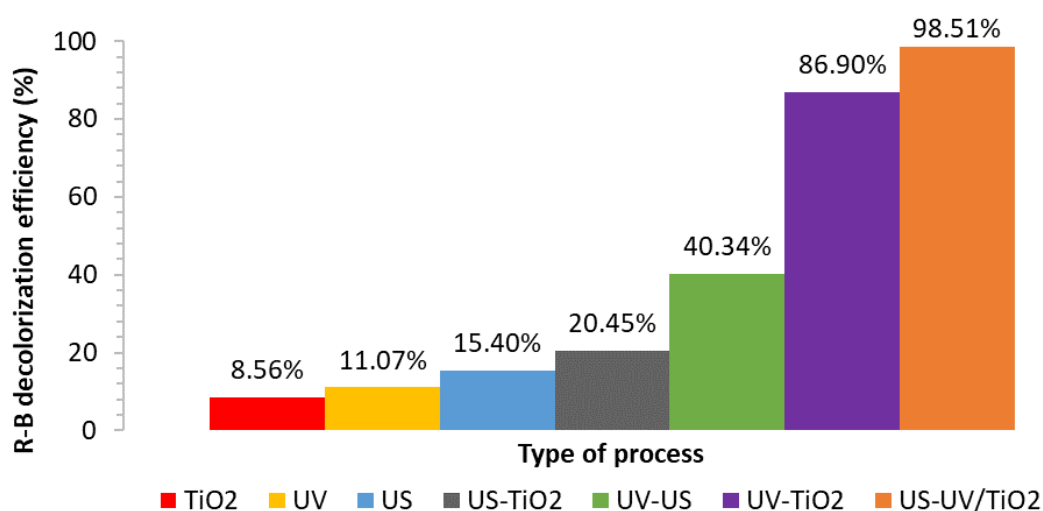


Figure 3. The decolorization performances of RhB using various processes. Experiment conditions: 20 mg/L RhB, 1.5 g/L catalyst concentration, and pH 5

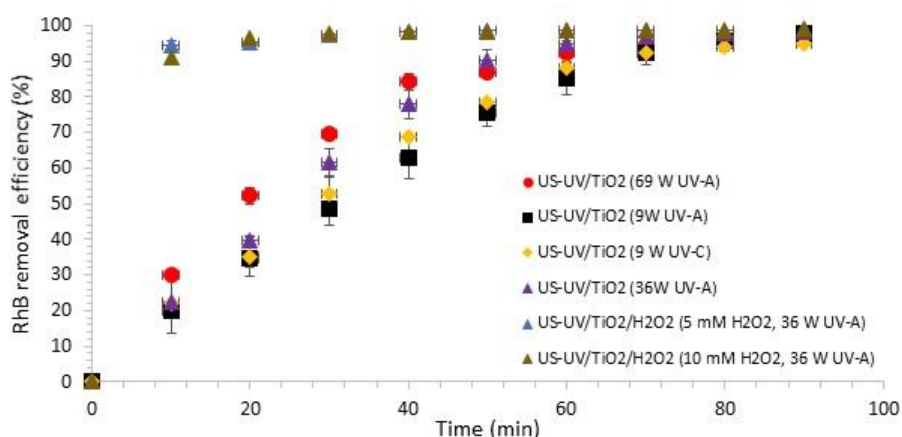


Figure 4. The decolorization of RhB dye in the presence of different lamp type, lamp electrical power and H₂O₂ concentrations. Reaction conditions: 15.25 mg/L RhB, 0.5 g/L catalyst loading, and pH 2

A synergy value >1.0 shows that hybrid SPC method has a synergistic impact on RhB decolorization compared with the individual process [26]. It is thought that the cavitation phenomenon may help higher mass transfer. Surface area and catalytic activity are also increased due to disaggregation of the photocatalyst particles. Hence, the synergistic effect is supported by the contribution of ultrasonic waves [37].

B. BBD ANALYSIS AND STATISTICAL DESIGN

As presented in Table 2, experimental and predicted values are considerably close to each other that demonstrates an interaction between modeled and actual decolorization of RhB dye depend on BBD-RSM strategy [38].

A quadratic polynomial equation was developed to achieve optimum decolorization efficiency of RhB dye owing the individual and collaborative interactions between three independent variables was developed [26]:

Efficiency of RhB decolorization (Y):

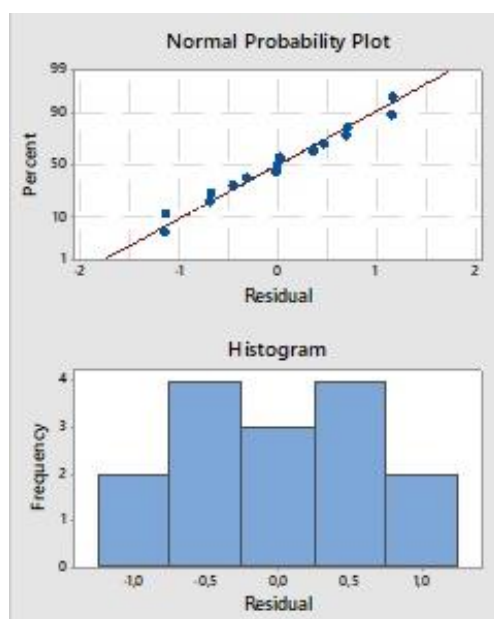
$$Y = 101,88 + 0,55 x_1 - 2,514 x_2 + 0,290 x_3 - 0,799 x_1 * x_1 + 0,0654 x_2 * x_2 - 0,01392 x_3 * x_3 + 0,392 x_1 * x_2 - 0,1239 x_1 * x_3 + 0,07147 x_2 * x_3; (R^2=0.9902, p<0.05). \quad (4)$$

C. ANALYSIS OF VARIANCE RESULTS OF THE MODEL

Probability values (p-values) were used to determine the significance of each factor coefficient as presented in Table 3. P < 0.05 means the factor is significant while p > 0.05 means non-significance at 95% confidence interval [39]. In this study, the ANOVA results of the second order polynomial equation model was investigated to obtain F and p values which were 56.02, 0.000, respectively. This implies that model is considerably significant (p<0.05). The changes of terms X₁², X₂² and X₁X₂ would not significantly affect the decolorization efficiency of RhB, since their p values that were lower than 0.05. In this study, the coefficient of determination is 0.9902 which indicates that the model exhibits the best fit. The adequacy of the model was confirmed based on the close R² adjusted (0.9725) and corresponding R² values similar to Assassi *et al.* [40]. Lack-of-fit F-value was 22.56 (p value, 4.30%) for the model.

Table 3. ANOVA results of the RhB decolorization (Y)

Source	Sum of squares	Degree of freedom	Mean square	F value	p value
Model	791.462	9	87.94	56.02	0.000
x_1 , TiO ₂	82.626	1	82.626	52.64	0.001
x_2 , pH	128.721	1	128.721	82	0.000
x_3 , RhB	291.611	1	291.611	185.78	0.000
x_1^2	2.358	1	2.358	1.5	0.275
x_2^2	4.039	1	4.039	2.57	0.170
x_3^2	114.416	1	114.416	72.89	0.000
x_1x_2	9.86	1	9.86	6.28	0.054
x_1x_3	24.552	1	24.552	15.64	0.011
x_2x_3	130.759	1	130.759	83.3	0.000
Lack of fit	7.848	3	2.541	22.56	0.043
Pure error	0.225	2	0.113		
Total	799.311	14			
$R^2=0.9902$		$R^2_{(pred)}=0.8468$		$R^2_{(adj)}=0.9725$	

**Figure 5.** Residual plot of model for percentage RhB decolorization

A normal probability plot and histogram of the residual for the decolorization of RhB are illustrated in Figure 5. The obtained results were confirmed by the accuracy of the model to predict RhB dye decolorization and residual independence [41]. The residuals were in the proximity of straight diagonal line that was shown in histogram diagram [21]. Therefore, in the present study, histogram showed normal distribution and the developed model was satisfied due to lower residuals for prediction of the decolorization efficiency of RhB.

D. ANALYSIS OF VARIANCE RESULTS OF THE MODEL

Ultrasonic decolorization of RhB solutions caused to an exponential decrease in the dye decolorization with time. The phenomenon of sonophotocatalytic decolorization of RhB could be expressed in a better way by using a kinetic study based on the Langmuir-Hinshelwood (L-H) reaction in the following equation [42]:

$$r = \frac{dC}{dt} = \frac{k_r KC}{1+KC} \quad (5)$$

where r is the rate of SPC decolorization (mg/minL); C is the RhB concentration at a time t (mg/L); K is adsorption coefficient; and k_r is kinetic constant of the reaction.

The Langmuir–Hinshelwood equation becomes [43]:

$$r = -\frac{dC}{dt} = k_r KC = K_{app} * t \quad (6)$$

The apparent degradation constant (K_{app} (min^{-1})) was calculated from the slope of the line of $\ln(C/C_0)$ as a function of time as shown in Table 4. Further, the half-life times were calculated by the following equation for a pseudo-first-order reaction:

$$t_{1/2} = -\frac{\ln 2}{K_{app}} \quad (7)$$

Table 4. Kinetic parameters for the RhB degradation

C_0 (mg/L)	r_0 (mg/Lmin)	k_{app} (1/min)	$t_{1/2}$ (min)	R^2	k_c (mg/Lmin)	K_{LH} (L/mg)
10	0.524	0.0524	13.23	0.9831		
15.25	0.72285	0.0474	14.62	0.9528		
30	0.873	0.0291	23.82	0.9806		
50	0.9	0.0180	38.51	0.9941		
					0.941	0.129

E. OPTIMIZATION AND VALIDATION

The 3D response surface and 2D contour plots visualize the synergistic effects between independent variables (X_1 , X_2 and X_3) and responses (Y) [41].

According to quadratic model that was obtained by the relationship between independent variables and response, absolute values of the coefficients in Equation 4 showed the magnitude of the effect, and the “+ and -” signs before the coefficients indicated whether the effect was positive or negative [42]. The negative coefficients for the model components X_2 , X_1^2 , X_3^2 , and X_1X_3 indicated the antagonistic effects on the RhB decolorization. While, the positive coefficients for X_1 , X_3 , X_1X_2 , X_2X_3 and X_2^2 indicated favorable effects on the RhB decolorization. The main individual effects as shown in Figure 6, demonstrated that pH had an adverse effect on the RhB decolorization efficiency, where decolorization increased with the decrease in the pH, whereas the TiO_2 concentration and RhB concentration had a favorable effect on the process, where RhB decolorization was improved with larger values of this parameters. For the model, all the optimum operating conditions were found at lowest values (0.5 g/L, 2 and 15.25 mg/L for TiO_2 concentration, pH and RhB concentration, respectively). For this reason, the highest value of all parameters could limit the decolorization performance. The interactions between the

TiO₂ concentration and pH, RhB concentration and pH had a favorable effect on response, but the interaction between RhB and TiO₂ concentrations had no extensive effect on the decolorization of RhB.

E. 1. PH EFFECT

The plots of response RhB decolorization efficiency as a function of the TiO₂ concentration and pH, while RhB concentration was fixed at 30 mg/L was illustrated in Figure 6(a1) and Figure 6(a2). It indicated that decreasing the TiO₂ concentration and pH leads to increase RhB decolorization efficiency. Acidic pH level supported exceptional decolorization of RhB than basic pH level; the optimum degradation was obtained at pH 2 after 90 min of working period. The physical and chemical properties of solution that affect the bubble dynamic is determined by pH. In higher pH, RhB could exist as ionic form and its diffusion is restricted into bubble-liquid interface. Thus, degradation of RhB could be occurred only in the interface that resulted with reduced decolorization efficiency [43].

Secondly, cationic (RhB⁺) and zwitterionic form (RhB[±]) are two principal forms in polar solvents. When pH value is higher than pKa of RhB (3.7 [44]), the carboxyl group is cationic (RhB⁺) or in zwitterionic form (RhB[±]). The carboxyl group of cationic form (RhB⁺) is deprotonated and the dye is transformed into zwitterionic form (RhB[±]), when the pH value is higher than pKa of RhB [45]. In other words, RhB has positive charge at low pH and negative charge at high pH due to its amphoteric nature [18]. At lower pH conditions, the hydrophilic character of RhB is lowest where the compound is in its cationic form and the degradation rate of RhB is maximum at the low pH. In strong acidic pH, RhB exists in higher concentrations at the bubble interface. Hence, the dye molecule is more exposed to the OH radical attack [47]. Furthermore, [46] supported the findings that the decrease in the degradation for higher pH values than pKa of RhB (3.7) is due to increase in the hydrophilic character of RhB as a result of dissociation of the molecule that lead to retard RhB molecular diffusion into the reaction zone. So, at this bubble interface, the uncombined OH radicals become maximum. For sonication, many researchers have already found that decrease in the solution pH leads to increase the sonochemical degradation rate due to formation of free radical scavengers (i.e. CO₃²⁻) which results in a decrease in the concentration of •OH at higher pH value [20].

E. 2. TiO₂ CATALYST CONCENTRATION EFFECT

It was considered that the nano-sized TiO₂ catalyst concentration could affect the decolorization of dye pollutant via adsorption and oxidation. The synergy of TiO₂ and initial RhB concentrations at a constant pH for RhB decolorization was given in Figure 6(b1) and 6(b2). The decolorization performance of RhB improved at the low level of RhB concentration; but the RhB concentration increased when the RhB decolorization efficiency decreased with increasing TiO₂ concentration. Besides, the synergy between TiO₂ (X₁) and initial RhB concentration (X₃) indicated a negative coefficient, which could indicate an adverse effect of X₁X₃ interaction on RhB decolorization. Increasing RhB dye concentration leads to mass transfer limitations and constant OH⁻ production that resulted with low decolorization efficiency [48].

Photons-embedded light that is emitted from UV light hits the surface of the catalyst and free electrons and protons are generated that are resulted from charge separation of TiO₂. These charge separation enables the degradation of RhB decolorization. Besides, hydroxyl radicals are generated from free electrons that react with oxygen molecules. Likewise, hydroxyl radicals can be generated from water molecules resulted from oxidation of dye molecules [31]. This phenomenon is thought to enhance the SPC decolorization of RhB pollutant in the aqueous media. Besides, the nucleation location of cavitation bubbles increases due to increased nanoparticle concentration. This leads to the increase of RhB degradation [18]. However, TiO₂ concentration of more than optimal 0.5 g/L, the specific activity of the catalyst is decreased due to particle aggregation, light scattering, and screening effects [49]. Similar behavior of the TiO₂ particles, has also been reported [18], dealing with degradation of RhB at the 0.5 g/L of TiO₂. [19] studied on the sonophotocatalysis of RhB decolorization with TiO₂ nanocatalyst in the range of 0.1 to 2 g/L and the optimum catalyst concentration for RhB decolorization was obtained at 0.5 g/L. They explained that the number of catalyst particle would not be sufficient to originate the primary

reaction at low TiO₂ concentration. Hence, 0.5 g/L of TiO₂ concentration was accepted as the optimum catalyst concentration for RhB decolorization by hybrid SPC process.

E. 3. RHB DYE DOSAGE EFFECT

Figures 6(c1) and 6(c2) presents the effect of initial RhB concentration and pH and their synergic relations on the RhB decolorization at TiO₂ concentration of 1.5 g/L. The RhB decolorization efficiency reached a maximum degradation while the pH value and initial RhB concentration approached to 2.0 and 20 mg/L, respectively.

The experiments were conducted for 10, 20, 30, 40, 50 mg/L RhB dye to evaluate the effectiveness of SPC decolorization performance as shown in Figure 6(b1-b2) and Figure 6(c1-c2). The decolorization of RhB dye decreased along with an increase in dye concentration as similar as many studies in the literature [20, 28]. The main reasons of the obtained results are the accumulation of dye molecules at the cavity interface and OH radicals show a great tendency to react with the pollutant molecule [20]. However, when RhB dye concentration increased, limited active sections could be available for the same TiO₂ concentration that resulted with less RhB molecular affection by OH [50]. It was further considered that, as the initial RhB concentration increased, higher concentration of intermediates was formed that competed with RhB for OH radicals. However, at the certain RhB concentration, organic dye molecules adhered to the surface of solid nanoparticles that affected the nucleation of cavitation bubbles, thus degradation efficiency was reduced [18]. Similar results have been reported for the case of ultrasound assisted degradation by [10]. Similar to our findings, [46] showed in their study that increasing initial RhB concentration from 5.95 mg/L to 12.5 mg/L and its intermediates at the bubble-liquid interface could lead to limit RhB degradation by the available interfacial area and OH radicals. [20] showed that almost complete decolorization (94%) of RhB was obtained after 1 h of irradiation under sonication at 10 mg/L of RhB concentration. When RhB concentration was below 10 mg/L, 100% RhB decolorization was achieved, thus optimum RhB dye concentration was accepted as 10 mg/L for RhB decolorization by hybrid SPC process.

According to the obtained results, it can be concluded that considering decolorization efficiency, the optimum values of these parameters for the SPC system were 0.5 g/L TiO₂ concentration, pH 2 and 15.25 mg/L RhB dye concentration. In order to validate the model prediction, the RhB decolorization performance was tested experimentally under optimum conditions. 98.5% of RhB decolorization efficiency was achieved under the optimum operating conditions, which confirmed the results of the developed model (99% decolorization efficiency). As shown in Table 5, the decolorization kinetics of RhB by SPC process is comparable to other advanced oxidation methods that performed almost complete RhB dye decolorization. In this study, levels of the independent variables were chosen at the most extensive ranges due to ease of operation and to get a knowledge about the interaction of different variables in the extensive perspective according to literature review. For instance, [51] already informed that the degradation efficiency of RhB was much slower in basic conditions (pH 8 and pH 10) than at acid medium (pH 6, 4 and 2) by sonocatalytic degradation using TiO₂. However, the necessity of examining the decolorization performances of RhB at higher and lower variable's levels cannot be ignored in the next studies.

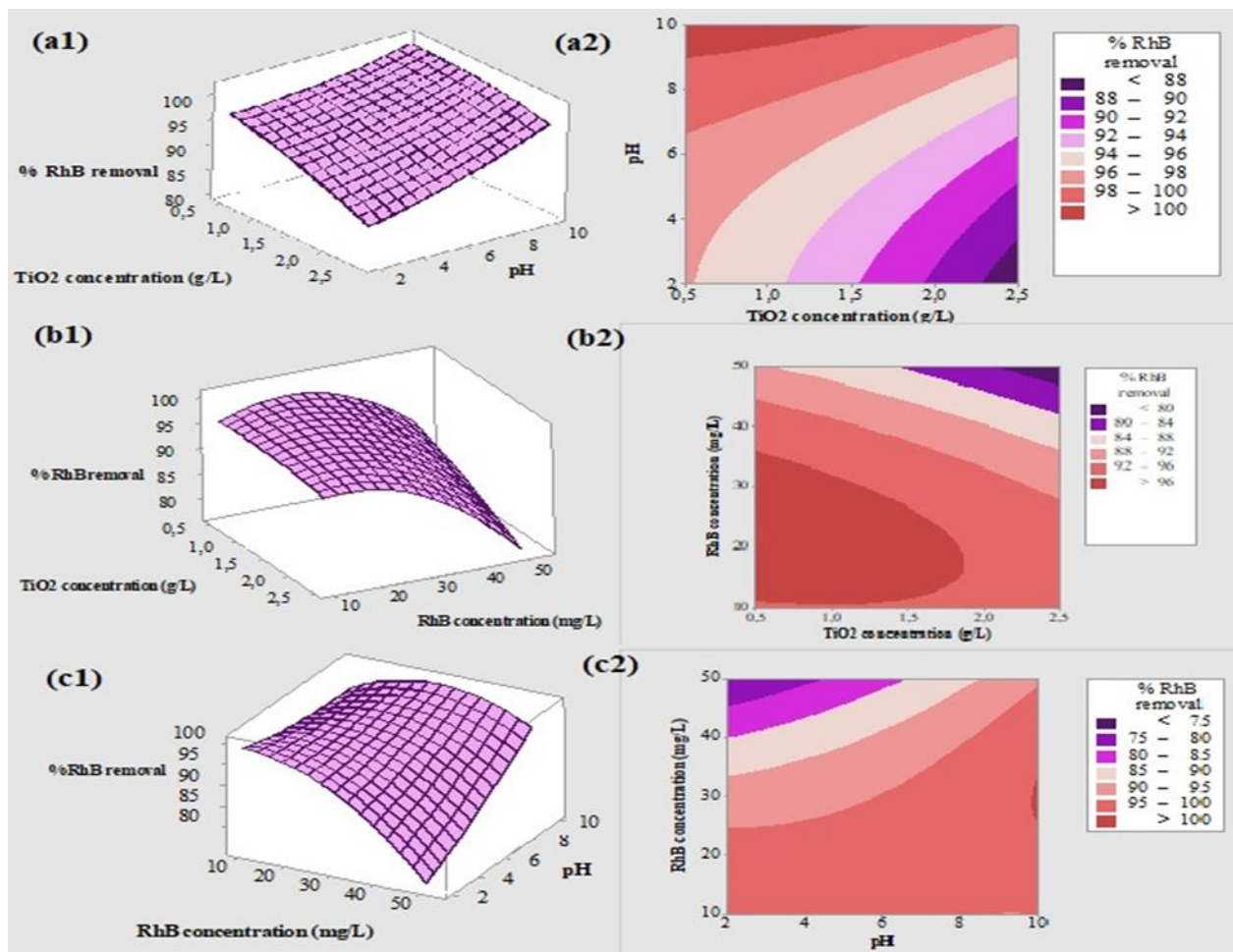


Figure 6. Surface and counter plots for RhB decolorization in 90-min by US-UV/TiO₂ system. Hold values are: a1–a2 [RhB]: 30 mg/L, b1–b2 [pH]: 6, c1–c2 [TiO₂]: 1.5 g/L

Table 5. Comparison of RhB decolorization efficiencies between SPC and other AOPs in the literature

Catalyst dosage	Pollutant concentration	Removal efficiency	Power	Time (min)	Kinetic rate (min ⁻¹)	References
TiO ₂ 0.5 g/L	RhB 10 mg/L	99%	UV=36 W US=120 W	90	0.0174	Present study
ZnO 1 g/L	RhB 100 mg/L	54%	UV=24 W	120	0.007	[52]
Na ₂ S ₂ O ₈ 20mM	RhB 10 mg/L	85%	US=60 W	60	-	[17]
1 wt% Ag doped on TiO ₂ 15mg/L	RhB 10 mg/L	90%	UV=250 W	60	0.036	[53]
TiO ₂ 2 g/L	RhB 10 mg/L	93%	UV=11 W US=1000 W	180	0.0162	[20]
TiO ₂ 0.5 g/L	RhB 20 mg/L	99%	US=300 W	40	-	[18]
TiO ₂ 0.3 g/L	RhB 10 mg/L	85%	UV US=170 W	180	8.6*10 ³	[10]

TiO ₂ NTs 2g/L	RhB 50 mg/L	85%	US=50 W	120	0.015	[54]
------------------------------	-------------	-----	---------	-----	-------	------

IV. CONCLUSION

The key findings of this study could be summarized as:

1) The calculated synergy value (2.42) indicated that the hybrid SPC method had a synergistic impact on RhB decolorization compared with the individual process and hybrid US-UV/TiO₂ system is an efficient and feasible technique to treat a type RhB containing wastewater compared to individual AOPs process;

2) A good compliance between experimental results and predictive values were obtained by the regression analysis for the model with R² value of 0.9902;

3) Based on ANOVA analysis, concentration of RhB stated the most significant effects (F=185.78) followed by pH (F= 82) and TiO₂ concentration (F=52.64) on the model;

4) Adding of H₂O₂ regardless of its concentration into the SPC process maximized the decolorization efficiency in a short time compared with US/UV-TiO₂ system regardless of its concentration. Likewise, higher lamp electrical power enhanced the degradation of RhB in a short working period regardless of lamp type;

5) Optimum parameters were obtained as 0.5 g/L of TiO₂, pH 2 and 10 mg/L of RhB, respectively. Further studies target the investigation of the independent variables effects on decolorization efficiency of RhB dye lower than mentioned optimum values found by SPC method;

6) The polynomial model indicated that decolorization of RhB was predicated as 98.5% at optimum conditions which was also confirmed by the validation study;

7) the Langmuir–Hinshelwood (L-H) model could strongly clarify the SPC process well, where k_c and K_{LH} were 0.941 mg/Lmin and 0.129 L/mg, respectively.

Consequently, less experiments and short time are the fundamental advantages in this approach to attain targeted information. Further studies need to apply this new combined system for pilot scale wastewater treatment.

ACKNOWLEDGEMENTS: This work was partially supported financially by the BAIBU Scientific Research Project Number:2021.09.02.1498. The author Gamze Dogdu contributed to the conception and design, conducting the experiment; acquisition, analysis, and interpretation of the data; and writing of the article. Nazmiye Ebru Şen and Simge Dalkılıç were gratefully acknowledged by the author for their invaluable helps in running experiments.

V. REFERENCES

[1] R. Wang, M. Shi, F. Xu, Y. Qiu, P. Zhang, K. Shen, Q. Zhao, J. Yu and Y. Zhang, “Graphdiyne-modified TiO₂ nanofibers with osteoinductive and enhanced photocatalytic antibacterial activities to prevent implant infection,” *Nature Communications*, vol. 11, pp. 4465, 2020.

- [2] Uludağ İhracatçı Birlikleri Genel Sekreterlikleri Ar-Ge Şubesi. "Türkiye Tekstil Sektörü ve Bursa." https://uib.org.tr/tr/kbfile/turkiye_tekstil_sektoru_ve_bursa_ocak_2020 (accessed Jan. 21, 2020).
- [3] V. B. K. S. Mullapudi, A. Salveru and A. J. Kora, "An in-house UV-photolysis setup for the rapid degradation of both cationic and anionic dyes in dynamic mode through UV/H₂O₂-based advanced oxidation process," *International Journal of Environmental Analytical Chemistry*, pp. 1-17, 2020.
- [4] A. Selim, S. Kaur, A.H. Dar, S. Sartaliya and G. Jayamurugan, "Synergistic effects of carbon dots and palladium nanoparticles enhance the sonocatalytic performance for rhodamine B degradation in the absence of light," *ACS Omega*, vol. 5, pp. 22603–22613, 2020.
- [5] Y. S. Lai, P. Parameswaran, A. Li, A. Aguinaga and B. E. Rittmann, "Selective fermentation of carbohydrate and protein fractions of *Scenedesmus*, and biohydrogenation of its lipid fraction for enhanced recovery of saturated fatty acids," *Biotechnology and Bioengineering*, vol. 113, pp. 320-329, 2016.
- [6] T. B. T. Dao, T. T. L. Ha, T. D. Nguyen, H. N. Le, C. N. Ha-Thuc, T. M. L. Nguyen, P. Perre and D. M. Nguyen, "Effectiveness of photocatalysis of MMT-supported TiO₂ and TiO₂ nanotubes for rhodamine B degradation," *Chemosphere*, vol. 280, pp. 130802, 2021.
- [7] C. Lops, A. Ancona, K. Di Cesare, B. Dumontel, N. Garino, G. Canavese, S. Hernández and V. Cauda, "Sonophotocatalytic degradation mechanisms of Rhodamine B dye via radicals generation by micro- and nano-particles of ZnO," *Applied Catalysis B: Environmental*, vol. 243, pp. 629-640, 2019.
- [8] P. Razaghi, K. Dashtian, F. Yousefi, R. Karimi and M. Ghaedi, "Gold anchoring to CuFe₂F₈(H₂O)₂ oxyfluoride for robust sono-photodegradation of Rhodamine-B," *Journal of Cleaner Production*, vol. 313, pp. 127916, 2021.
- [9] H. Selcuk, "Decolorization and detoxification of textile wastewater by ozonation and coagulation processes," *Dyes and Pigments*, vol. 64, pp. 217-222, 2005.
- [10] S. P. Hinge, M. S. Orpe, K. V. Sathe, G. D. Tikhe, N. S. Pandey, K. N. Bawankar, M. V. Bagal, V. G. Mohod and R. Parag, "Combined removal of Rhodamine B and Rhodamine 6G from wastewater using novel treatment approaches based on ultrasonic and ultraviolet irradiations," *Desalination and Water Treatment*, vol. 3994, pp. 0-13, 2016.
- [11] P. R. Gogate, M. Sivakumar, and A. B. Pandit, "Destruction of Rhodamine B using novel sonochemical reactor with capacity of 7.5 l," *Separation and Purification Technology*, vol. 34, pp. 130-24, 2004.
- [12] E. Adamek, W. Baran, J. Ziemiańska, and A. Sobczak, "The Comparison of Photocatalytic Degradation and Decolorization Processes of Dyeing Effluents," *International Journal of Photoenergy*, pp. 578191, 2013.
- [13] D. Pratiwi, A. W. Indrianingsih, C. Darsih, and Hernawan, "Decolorization and Degradation of Batik Dye Effluent using *Ganoderma lucidum*," *IOP Conf. Series: Earth and Environmental Science*, vol. 101, pp. 012034, 2017.
- [14] J. A. Ayala, C. O. Castillo and R. S. Ruiz, "Ultrasonic, ultraviolet, and hybrid catalytic processes for the degradation of rhodamine B dye: Decolorization kinetics," *Revista Mexicana de Ingeniera Quimica*, vol. 16, 521-529, 2017.

- [15] K. Soutsas, V. Karayannis, I. Poullos, A. Riga, K. Ntampeglitis, X. Spiliotis, and G. Papapolymerou, "Decolorization and degradation of reactive azo dyes via heterogeneous photocatalytic processes," *Desalination*, vol. 250, 345-350, 2010.
- [16] T. Rasheed, M. Bilal, H. M. N. Iqbal, S. Z. H. Shah, H. Hu, X. Zhang, and Y. Zhou, "TiO₂/UV-assisted rhodamine B degradation: putative pathway and identification of intermediates by UPLC/MS," *Environmental Technology*, vol. 39, 1533-1543, 2018.
- [17] P. Zawadzki, "Comparative studies of Rhodamine B decolorization in the combined process Na₂S₂O₈/visible light/ultrasound," *Desalination and Water Treatment*, vol. 213, pp. 269-278, 2021.
- [18] D. Xu and H. Ma, "Degradation of rhodamine B in water by ultrasound-assisted TiO₂ photocatalysis," *Journal of Cleaner Production*, vol. 313, pp. 127758, 2021.
- [19] F. Ahmedchekkat, M.S. Medjram, M. Chiha and A.M. Ali Al-bsoul, "Sonophotocatalytic degradation of Rhodamine B using a novel reactor geometry: effect of operating conditions," *Chemical Engineering Journal*, vol. 178, pp. 244-251, 2011.
- [20] K. P. Mishra and P. R. Gogate, "Intensification of degradation of aqueous solutions of rhodamine B using sonochemical reactors at operating capacity of 7 L," *Journal of Environmental Management*, vol. 92, pp. 1972-1977, 2011.
- [21] P. Singh, A. Dhir and V. K. Sangal, "Optimization of Photocatalytic Process Parameters for the Degradation of Acrylonitrile Using Box Behnken Design," *Desalination and Water Treatment*, 55, 1501-1508, 2015.
- [22] G. E. P. Box, W. G. Hunter and J. S. Hunter, "Statics for Experiments: An Introduction to Design Data Analysis and Model Building", Wiley: New York, 1978.
- [23] J. Abdi, A. Jamal Sisi, M. Hadipoor, and A. Khataee, "State of the art on the ultrasonic-assisted removal of environmental pollutants using metal-organic frameworks," *Journal of Hazardous Materials*, 424, 127558, 2022.
- [24] S. Moradi, S. A. Sobhgol, F. Hayati, A.A. Isari, B. Kakavandi, P. Bashardoust and B. Anvaripour, "Performance and reaction mechanism of MgO/ZnO/Graphene ternary nanocomposite in coupling with LED and ultrasound waves for the degradation of sulfamethoxazole and pharmaceutical wastewater," *Separation and Purification Technology*, vol. 251, pp. 117373, 2020.
- [25] S. D. Ayare and P. R. Gogate, "Sonophotocatalytic oxidation based treatment of phthalocyanine pigment containing industrial wastewater intensified using oxidising agents," *Separation and Purification Technology*, vol. 233, pp. 115979, 2020.
- [26] H. Wei, MdH. Rahaman, J. Zhao, D. Li and J. Zhai, "Hydrogen peroxide enhanced sonophotocatalytic degradation of acid orange 7 in aqueous solution: optimization by Box-Behnken design," *Journal of Chemical Technology and Biotechnology*, vol. 96, pp. 2647-2658, 2021.
- [27] S.G. Babu, P. Karthik, M.C. John, S.K. Lakhera, M. Ashokkumar, J. Khim and B. Neppolian, "Synergistic effect of sono-photocatalytic process for the degradation of organic pollutants using CuO-TiO₂/Rgo," *Ultrasonic Sonochemistry*, vol. 50, pp. 218-223, 2019.
- [28] G. Dogdu Okcu, T. Tunacan and E. Dikmen, "Photocatalytic degradation of yellow 2G dye using titanium dioxide/ultraviolet A light through a Box-Behnken experimental design: Optimization and kinetic study," *Journal of Environmental Science and Health - Part A Toxic/Hazardous Substances and Environmental Engineering*, vol. 54, pp. 136-145, 2019.

- [29] H. Chaker, N. Ameer, K. Saidi-Bendahou, M. Djennas and S. Fourmentin, "Modeling and Box-Behnken design optimization of photocatalytic parameters for efficient removal of dye by lanthanum-doped mesoporous TiO₂," *Journal of Environmental Chemical Engineering*, vol. 9, pp. 104584, 2021.
- [30] F. S. Domingues, H. C. L. Geraldino, T. K. F. de Souza Freitas, C. A. de Almeida, F. F. de Figueiredo, and J. C. Garcia, "Photocatalytic degradation of real textile wastewater using carbon black-Nb₂O₅ composite catalyst under UV/Vis irradiation," *Environmental Technology*, vol. 42, pp. 2335–2349, 2021.
- [31] M. Kaur, A. Noonaa, A. Dogra and P. Singh Thind, "Optimising the parameters affecting degradation of Cypermethrin in an aqueous solution using TiO₂/H₂O₂ mediated UV photocatalysis: RSM-BBD, kinetics, isotherms and reusability," *International Journal of Environmental Analytical Chemistry*, pp. 1-15, 2021.
- [32] J. Wang, Z. Jiang, Z. Zhang, Y. Xie, X. Wang, Z. Xing, R. Xu, and X. Zhang, "Sonocatalytic degradation of acid red B and rhodamine B catalyzed by nano-sized ZnO powder under ultrasonic irradiation," *Ultrasonics Sonochemistry*, vol. 15, pp. 768-774, 2008.
- [33] M. Inoue, F. Okada, A. Sakurai, and M. Sakakibara, "A new development of dyestuffs degradation system using ultrasound," *Ultrasonics Sonochemistry*, vol. 13, pp. 313-320, 2006.
- [34] V. Katheresan, J. Kansedo and S.Y. Lau, "Efficiency of various recent wastewater dye removal methods: A review," *Journal of Environmental Chemical Engineering*, vol. 6, pp. 4676-4697, 2018.
- [35] S. Rahimi, B. Ayati and A. Rezaee, "Optimization of reaction parameters for the sonophotocatalytic degradation of hydroquinone," *Research on Chemical Intermediates*, vol. 43, pp. 1935-1956, 2017.
- [36] Y. He, F. Grieser and M. Ashokkumar, "Kinetics and mechanism for the sonophotocatalytic degradation of p-chlorobenzoic acid," *The Journal of Physical Chemistry A*, vol. 115, pp. 6582–6588, 2011.
- [37] S. Mosleh, M.R. Rahimi, M. Ghaedi and K. Dashtian, "Sonophotocatalytic degradation of trypan blue and vesuvine dyes in the presence of blue light active photocatalyst of Ag₃PO₄/Bi₂S₃-HKUST-1-MOF: central composite optimization and synergistic effect study," *Ultrasonic Sonochemistry*, vol. 32, pp. 387–397, 2016.
- [38] G. Asgari, A. Shabanloo, M. Salari and F. Eslami, "Sonophotocatalytic treatment of AB113 dye and real textile wastewater using ZnO/persulfate: Modeling by response surface methodology and artificial neural network," *Environmental Research*, vol. 184, pp. 109367, 2020.
- [39] I. Arslan-Alaton, G. Tureli and T. Olmez-Hanci, "Treatment of azo dye production wastewaters using photo-Fenton-like advanced oxidation processes: Optimization by response surface methodology," *Journal of Photochemistry and Photobiology A: Chemistry*, vol. 202, pp. 142–153, 2009.
- [40] M. Assassi, F. Madjene, S. Harchouche and H. Boulfiza, "Photocatalytic treatment of Crystal Violet in aqueous solution: Box–Behnken optimization and degradation mechanism," *Environmental Progress and Sustainable Energy*, pp. 1-8, 2021.
- [41] A.H. Jawad, N.N.A. Malek, A.S. Abdulhameed and R. Razuan, "Synthesis of magnetic chitosan-fly ash/Fe₃O₄ composite for adsorption of reactive orange 16 dye: optimization by Box–Behnken design," *Journal of Polymers and the Environment*, vol. 28, pp. 1068–1082, 2020.
- [42] B. Boutra and M. Trari, "Solar photodegradation of a textile azo dye using synthesized ZnO/bentonite," *Water Science and Technology*, vol. 75, pp. 1211–1220, 2017.

- [43] S. Mosleh, M.R. Rahimi, M. Ghaedi, A. Asfaram, R. Jannesar, and F. Sadeghfar, "A rapid and efficient sonophotocatalytic process for degradation of pollutants: Statistical modeling and kinetics study," *Journal of Molecular Liquids*, vol. 261, pp. 291–302, 2018.
- [42] A. Arslan, E. Topkaya, S. Veli and D. Bingöl, "Optimization of Ultrasonication Process for the Degradation of Linear Alkyl Benzene Sulfonic Acid by Response Surface Methodology," *Clean - Soil, Air, Water*, vol. 46, pp. 1700508, 2018.
- [43] Z. Zhang and H. Zheng, "Optimization for decolorization of azo dye acid green 20 by ultrasound and H₂O₂ using response surface methodology," *Journal of Hazardous Materials*, vol. 172, pp. 1388–1393, 2009.
- [44] N. Serpone, R. Terzian, H. Hidaka and E. Pelizzetti, "Ultrasonic induced dehalogenation and oxidation of 2-, 3-, and 4-chlorophenol in air-equilibrated aqueous media. Similarities with irradiated semiconductor particulates," *The Journal of Physical Chemistry A*, vol. 98, pp. 2634–2640, 1994.
- [45] S. Woislowski, "The spectrophotometric determination of ionization constants of basic dyes," *Journal of the American Chemical Society*, vol. 75, pp. 5201–5203, 1953.
- [46] O. Aguilar, C. Ángeles, C. O. Castillo, C. Martínez, R. Rodríguez, R. S. Ruiz, and M. G. Vizcarra, "On the ultrasonic degradation of Rhodamine B in water: kinetics and operational conditions effect," *Environmental Technology*, vol. 35, pp. 1183–1189, 2014.
- [47] S. Merouani, O. Hamdaoui, F. Saoudi and M. Chiha, "Sonochemical degradation of Rhodamine B in aqueous phase: Effects of additives," *Chemical Engineering Journal*, vol. 158, pp. 550-557, 2010.
- [48] D. Dimitrakopoulou, I. Rethemiotaki, Z. Frontistis, N. P. Xekoukoulotakis, D. Venieri and D. Mantzavinos, "Degradation, mineralization and antibiotic inactivation of amoxicillin by UV-A/TiO₂ photocatalysis," *Journal of Environmental Management*, vol. 98, pp. 168–174, 2012.
- [49] S. Bouafia-Chergui, H. Zemmouri, M. Chabani and A. Bensmaili, "TiO₂-Photocatalyzed Degradation of Tetracycline: Kinetic Study, Adsorption Isotherms, Mineralization and Toxicity Reduction," *Desalination and Water Treatment*, 57, 16670–16677, 2016.
- [50] S. J. Jafari, G. Moussavi and H. Hossaini, "Degradation and Mineralization of Diazinon Pesticide in UVC and UVC/TiO₂ Process," *Desalination and Water Treatment*, vol. 57, pp. 3782–3790, 2016.
- [51] Y. L. Pang, S. Bhatia, and A. Z. Abdullah, "Process behavior of TiO₂ nanotube-enhanced sonocatalytic degradation of Rhodamine B in aqueous solution," *Separation and Purification Technology*, vol. 77, pp. 331–338, 2011.
- [52] F. Madjene, M. Assassi, I. Chokri, T. Enteghar and H. Lebig, "Optimization of photocatalytic degradation of rhodamine B using Box – Behnken experimental design: Mineralization and mechanism," *Water Environment Federation*, vol. 93, pp. 112–122, 2021.
- [53] N. Chakinala, P.R. Gogate and A.G. Chakinala, "Photocatalytic degradation of rhodamine-B over mono- & bi-metallic TiO₂ catalysts," *Materials Today: Proceedings*, vol. 43, pp. 3066–3070 Contents, 2021.
- [54] Y.L. Pang, A.Z. Abdullah and S. Bhatia, "Review on sonochemical methods in the presence of catalysts and chemical additives for treatment of organic pollutants in wastewater," *Desalination*, vol. 277, pp. 1–14, 2011.